ELSEVIER

Journal of Magnetism and Magnetic Materials 192 (1999) 258–262

Journal of magnetism and magnetic materials

Magnetoresistance, magnetization and FMR study of Fe/Ag/Co multilayer film

C. Birlikseven[a], C. Topacli[a,*], H.Z. Durusoy[a], L.R. Tagirov[a,1], A.R. Koymen[b], B. Aktas[c]

[a]*Faculty of Engineering, Department of Physics, Hacettepe University, Beytepe 06532, Ankara, Turkey*
[b]*University of Texas at Arlington, Arlington, TX 76019, USA*
[c]*Gebze Institute for Advanced Technologies, 41410 Cayirova-Gebze/Kocaeli, Turkey*

Received 10 June 1998

Abstract

The polycrystalline $[Fe/Ag/Co/Ag] \times 3$ asymmetric multilayer film was prepared by the UHV magnetron sputtering method on silicon. In-plane magnetization measurements showed structured hysteresis loops. Magnetoresistance (MR) measurements revealed giant magnetoresistance effect with magnitudes in 0.14–0.21% range at room temperature. The saturation magnetizations and the interaction between layers were studied by ferromagnetic resonance and revealed an indistinguishably weak interlayer coupling from out-of-plane geometry of measurements. The MR data are interpreted based on incomplete domain alignment model for polycrystalline magnetic films.

PACS: 75.60; 75.70

Keywords: FMR; GMR; Magnetic films; Magnetization

1. Introduction

There has been a great interest to investigate the magnetoresistance of multilayers composed of Fe-, Ni- and Co-based ferromagnets alternated with noble metals like Cu or Ag [1–6]. These multilayers, being the so-called uncoupled systems in the sense that the magnetic layers are not coupled by the conduction electron mediated exchange, nevertheless show an appreciable change of resistance up to few percents, which are commonly called giant magnetoresistance (GMR). The importance of the above systems is that they exhibit the GMR effect at small values of magnetic field (typically 5–50 G), which make them promising sensors for magnetic read–write head applications. In this paper we report the magnetoresistance, magnetization and ferromagnetic resonance (FMR) studies of the polycrystalline $[Fe(20\,\text{Å})/Ag(40\,\text{Å})/Co(20\,\text{Å})/Ag(40\,\text{Å})] \times 3$ multilayer films at room temperature.

* Corresponding author. Tel.: + 90 4 235 25 51; fax: + 90 4 235 25 50.

[1] On leave from Kazan State University, Kazan 420008, Tatarstan, Russian Federation.

0304-8853/99/$ – see front matter
PII: S0304-8853(98)00302-3

2. Results

2.1. Sample preparation

The films were deposited by DC magnetron sputtering method on single crystalline Si(1 0 0) substrate in a UHV system at room temperature with growing rate of about 0.15 Å/s Ag layers of 20 Å thickness were used as buffer and top protective layers. Iron and cobalt layers were grown of 20 Å thickness, the Ag spacer layer was 40 Å thick to ensure the absence of conduction electron mediated exchange interaction between magnetic layers. Structural investigation made on the scanning electron microscope JEOL JEM-1200EX revealed the polycrystalline growth of the films with grain size $\sim$ 300–400 Å.

2.2. Magnetization

Magnetization measurements by a sensitive vibrating sample magnetometer (VSM) LakeShore 7300 were made with in-plane geometry for the magnetic field. They revealed the structured hysteresis loop shown in Fig. 1a. The rounded shape of the loop indicates the incomplete magnetic moment alignment within the layers because of mosaicity of in-plane easy-axes of crystallites, that is expected for our polycrystalline films. The coercivity field of the main step is $H_{c1} \simeq \pm 26$ G, which we referred to the iron layers, is markedly smaller than the coercivity field for the 50 Å thick Fe layer in Ref. [5]. There are also three visible shoulders on higher fields, the central one of them has the coercivity field $H_{c2} \approx 90$ G, which is slightly smaller than that seen in the hysteresis loop for 50 Å thick Co layer presented in Ref. [5]. We attribute those features of the hysteresis loop to the responses of the Co layers of our triply repeated Fe/Ag/Co/Ag structure. Overall view of the magnetization loop is qualitatively similar to Ref. [5] and may be explained by the weighted superposition of hysteresis loops of each of the materials.

2.3. Magnetoresistance

The stripe-shaped samples with dimensions 100 μm × 3 mm were prepared by lithography technique with current and potential leads being attached by the springed contacts via the silver paint dots. The resistivity $R(H)$ of the samples in the magnetic field H was measured in standard in-plane geometry with current and magnetic field lying in the film plane being perpendicular to each other. The GMR MR(H) (percents) as a function of the field has been defined as

$$\mathrm{MR}(H) = \frac{R(H) - R(H_s)}{R(H_s)} \times 100, \quad (1)$$

where $H_s \simeq 500$ G is the saturation field. The results of the measurements are displayed on the panel (b) of Fig. 1. They clearly show hysteretic behavior of MR with the field for maximum derivative of MR(H) correlating closely with $H_{c1} \simeq \pm 26$ G obtained from the magnetization measurements (panel (a) of Fig. 1). The magnitude of the MR(H) results presented is about 0.21% for the unannealed sample. We have made the heat

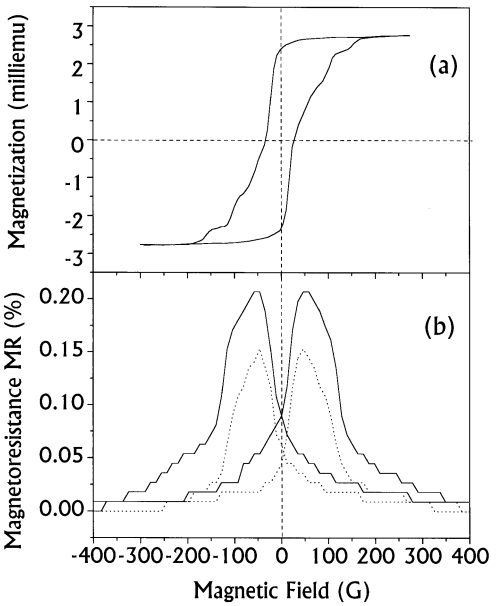

Fig. 1. VSM measured magnetization (panel (a)) and magnetoresistance MR(H) measurements (panel (b)) for [Fe(20 Å)/Ag(40 Å)/Co(20 Å)/Ag(40 Å)] × 3 multilayer films at room temperature. Solid curve on the panel (b) displays the MR results for unannealed sample, the dotted curve shows MR(H) after annealing in Ar(95%)H(5%) atmosphere at 300°C during 10 min.

treatment with our samples, according to Hylton et al. [3], but annealing did not lead to increase of the MR magnitude (see the dashed curve on Fig. 1b and figure caption). For our long-stripe samples we expect also the contribution of anisotropic magnetoresistance (AMR) to MR(H), that is why we have measured magnetoresistance with current and magnetic field being parallel to each other, but lying in the film plane. This resulted in approximately 30% reduction of MR(H) with respect to the previous case when current and magnetic field were perpendicular. This reduction may be considered as the estimate of AMR effect in our samples.

2.4. FMR

Ferromagnetic resonance experiments were carried out on BRUKER-EMX X-band ESR spectrometer at $\nu = 9.79$ GHz at room temperature. The samples were mounted on a goniometer which allowed them to rotate with 1.0° step in out-of-plane geometry with DC magnetic field changing its angle θ_H from the film normal ($\theta_H = 0$) to the film plane ($\theta_H = 90°$) and AC field lying always in the film plane. The measurements showed overlapped resonance lines in the main domain of measured angles, and two separate lines at angles close to the film normal. These two lines were attributed to the FMR signals coming from the Fe and Co layers constituting our multilayer system. We developed the computer procedures for the decomposition of the spectra to two lines, the results for the angular dependence of the resonance fields for the individual lines are shown on the panel (a) of Fig. 2 by solid square and opened circle symbols (see the figure caption). The linewidths for the resonance lines were: $\Delta H_{\mathrm{Co}} \simeq 587$ G and $\Delta H_{\mathrm{Fe}} \simeq 303$ G at $\theta_H = 0$, and $\Delta H_{\mathrm{res}} \simeq 101$ G for the overlapped line at $\theta_H = 90°$.

The FMR results are analyzed using a coordinate system in which θ is the polar angle measuring the deviation of magnetization vector $\boldsymbol{M}$ from the film normal. The free energy density is given by

$$E = -(\boldsymbol{M}\cdot\boldsymbol{H}) + (2\pi M^2 - K_{\mathrm{n}})\cos^2\theta + E_{\mathrm{anis}}, \quad (2)$$

which defines the effective magnetization

$$4\pi M_{\mathrm{eff}} = 4\pi M - 2K_{\mathrm{n}}/M. \quad (3)$$

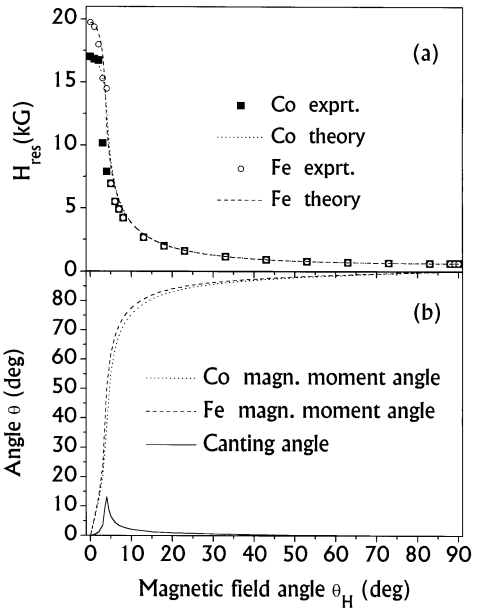

Fig. 2. FMR fields for resonance (panel (a)) and layers magnetizations and canting angles (panel (b)) versus angle of the DC magnetic field measured from the film normal. Panel (a) symbols show the experimental results, curves display the results of the theory. Panel (b) dashed and dotted curves show the equilibrium angles of magnetic moments with respect to the film normal, solid line gives the canting angle between magnetizations of Fe and Co layers.

Here K_{n} is uniaxial anisotropy normal to the film plane, M is the true saturation magnetization at current temperature, E_{anis} term may include any type of magneto-crystalline anisotropy, it was set to be equal to zero for our polycrystalline samples. The general ferromagnetic resonance condition [7] together with the condition for equilibrium, given by the zeros of the first angular derivatives of E with respect to the angle θ, determine the FMR resonance field H_{res} as a function of the angle θ_H. The effective magnetization $4\pi M_{\mathrm{eff}}$ can be obtained from the fitting of the calculated curve to the experiment. The results of the analysis are given on the upper panel of Fig. 2 by dashed and dotted lines, they show good agreement with experimental data. We obtained the values of the effective magnetizations of the layers: $(4\pi M_{\mathrm{eff}})_{\mathrm{Fe}} = 16.43$ kG and $(4\pi M_{\mathrm{eff}})_{\mathrm{Co}} = 13.94$ kG. The values $(\omega/\gamma)_{\mathrm{Fe}} \simeq 3.3294$ kG and $(\omega/\gamma)_{\mathrm{Co}} \simeq 3.0767$ kG have been

obtained upon fitting ($\omega = 2\pi v$, γ is the gyromagnetic ratio), which correspond to spectroscopic g-factors, $g_{Fe} \simeq 2101$ and $g_{Co} \simeq 2.2734$ for Fe and Co layers, respectively.

The calculations give the possibility to determine the equilibrium magnetization angle θ for each of the layers and canting angle between the magnetizations of Co and Fe layers as a function of the DC magnetic field angle θ_H. The results for the magnetization angles are displayed on the panel (b) of Fig. 2.

3. Discussion

Note first of all, that we have performed calculations as in Fig. 2 with the assumption that the magnetic layers are noninteracting. From the lower panel we can learn that in the field angle range 3–8°, the angle between magnetizations (canting angle), which is mainly due to different demagnetization fields, reaches its maximum value $\geqslant 13°$. If an appreciable magnetostatic interaction exists between canted magnetizations, then, according to our estimations, it should manifest itself by the appearance of resonances as the maximum canting angle is reached. The experimental data on angular dependence of the resonance field do not reveal the influence of interlayer interaction. Thus, we may conclude that the strength of the magnetostatic field is considerably lower than the FMR field for resonance.

The value for $4\pi M_{eff}$ of the iron layers differs markedly from the bulk value $\simeq 21.6$ kG at room temperature [8], quoted in Ref. [9], but according to their measurements on the single-crystal iron films on GaAs substrate with variable Fe layer thickness d_{Fe}, upon changing d_{Fe} from 120 Å down to 16 Å, $(4\pi M_{eff})_{Fe}$ decreased from $\simeq 17.5$ to $\simeq 7.5$ kG. Prinz et al. [9] attributed the experimentally observed reduction of the effective magnetization to the influence of perpendicular surface anisotropy, arising at the interface with substrate. In a recent investigation of the sputtered iron films on MgO substrate [10] a decrease of the effective $4\pi M$ from near the bulk value at the thickness $d_{Fe} = 500$ Å to $(4\pi M_{eff})_{Fe} \simeq 16.0$ kG at $d_m = 30$ Å was found. Goryunov et al. [10] (see also the review by Heinrich and Cochran [11]) have discussed in detail possible contributions of magnetostriction and Néel [12] mechanism to the uniaxial surface anisotropy. First one comes from the strain due to the lattice mismatch between the magnetic layer and the spacer (or substrate) and was found to be insufficient to explain the observed values of perpendicular anisotropy, as the bulk magnetoelastic coefficient has been used for the quantitative estimation. The Néel mechanism attributes the surface uniaxial anisotropy to arise from the abrupt breaking of local symmetry at the interface, and was found to give correct sign and order of magnitude, if the enhancement by the interface dislocations is taken into account. Another mechanism of $4\pi M$ reduction is the roughness of interface [13]. The magnetostatic energy associated with roughness always leads to reduction of effective $4\pi M$, it can be important for our samples, because the common roughness of the sputtered films of about two monolayers is comparable with total film thickness ~ 20 Å (6–7 monolayers). It is worth to note that Eq. (5) of Ref. [13] is not appropriate for quantitative estimations in the case of ultrathin films, because it is derived for the roughness much smaller than the film thickness. According to Eq. (3) the energy of effective uniaxial anisotropy being interpreted as the surface one $K_n = K_n^s/d_{Fe}$, can be estimated as $(K_n^s)_{Fe} \simeq 0.89$ erg cm^{-2} at $d_{Fe} = 20$ Å, which is close to the values 0.69 and 0.81 erg cm^{-2} for the Fe/Ag interfaces quoted in Table 1 of Ref. [11]. The value of g-factor $g_{Fe} \simeq 2.101$ is only slightly greater than the corresponding one for the bulk iron $g_{Fe} \simeq 2.09$ [8].

The value of $(4\pi M_{eff})_{Co} = 13.94$ kG for the cobalt layers also differs well from the bulk value $(4\pi M_{eff})_{Co} = 17.8$ kG [8]. In the investigation of Co films grown on MgO and Al_2O_3 substrates [14] a substantial reduction of the saturation moment upon decreasing the film thickness in the range 350–120 Å was found. According to Ref. [11] the uniaxial perpendicular anisotropy for Co layers in Co/Au and Co/Cu superlattices contains substantial constant (bulk) contribution and a surface term proportional to $1/d_{Co}$. As our samples have the constant thickness of Co layers, we restrict our estimation only by quoting the value of $(K_n)_{Co} \simeq 2.7 \times 10^6$ erg cm^{-3}. The value of g-factor $g_{Co} \simeq 2.2734$ lies

well beyond the quoted value $g \simeq 2.18$ for bulk hcp Co [8]. In a recent investigation of Co/Cr multilayers [15] with Co layers thicknesses t_{Co} around 20 Å the monotonous increase of g-factor value from $g_{Co_o} \simeq 2.20$ at $t_{Co} = 34$ Å to $g_{Co} \simeq 2.26$ at $t_{Co} = 12$ Å have been observed, which correlates with our observation of increased g-factor value for the thin Co film ($t_{Co} \simeq 20$ Å) with respect to the bulk value.

The magnetoresistance data can be qualitatively explained in the multidomain model with the existence of certain fraction of mutually oppositely oriented, counterpart domains in different layers [5]. There exist two configurations for the current flow across the layers: between two domains of opposite orientation and two domains of aligned orientation of magnetizations. If the domains are larger compared to mean spin scattering length and the spacer thickness, these two configurations will have essentially different resistivities. Then the magnetoresistance rises and drops will be confined to the coercivity fields at which the magnetizations of the layers experience reversal. Fig. 1 clearly confirms that physical picture: the maxima of the MR curve for the unannealed sample correspond to the magnetization reversal paths for the Fe layer magnetization. Moreover on the MR(H) curves, there clearly are the shoulder-like features, which we attribute to the reversal fields for the Co layers. We believe that the multidomain model adequately reflects the polycrystalline nature of our samples.

Acknowledgements

This work was supported by the Welch Foundation and Texas Higher Education Coordinating board. The research of L.R.T. at Hacettepe University, Ankara is supported by TÜBITAK within NATO-CPC AFP. C.T. and H.Z.D. acknowledge TÜBITAK for supporting the research through TBAG-1271 and NATO-B2.

References

[1] B. Dieny, V.S. Speriosu, S.S.P. Parkin, B.A. Gurney, D.R. Withoit, D. Mauri, Phys. Rev. B 43 (1991) 1297.
[2] W.R. Pratt Jr., S.-F. Lee, J.M. Slaughter, R. Lolee, P.A. Schroeder, J. Bass, Phys. Rev. Lett. 66 (1991) 3060.
[3] T.L. Hylton, K.R. Coffey, M.A. Parker, J.K. Howard, Science 261 (1993) 1021.
[4] D. Miyauchi, S. Araki, Appl. Phys. Lett. 63 (1993) 1702.
[5] Y.I. Idzerda, C.-T. Chen, S.F. Cheng, W. Vavra, G.A. Prinz, G. Meigs, H.-J. Lin, G.H. Ho, J. Appl. Phys. 76 (1994) 6525.
[6] C. Cowache, B. Dieny, A. Chamberod, D. Benizri, F. Berthet, S. Auffret, L. Giacomoni, S. Nossov, Phys. Rev. B 53 (1996) 15027.
[7] H. Suhl, Phys. Rev. 55 (1955) 555.
[8] Numerical Data and Functional Relationships in Science and Technology, Landolt-Börnstein, New Series, vol. III/19a, Springer, Heidelberg, 1986.
[9] G.A. Prinz, G.T. Rado, J.J. Krebs, J. Appl. Phys. 53 (1982) 2087.
[10] Yu.V. Goryunov, N.N. Garifyanov, G.G. Khaliullin, I.A. Garifullin, L.R. Tagirov, F. Schreiber, Th. Mühge, H. Zabel, Phys. Rev. B 52 (1995) 13450.
[11] B. Heinrich, J.F. Cochran, Adv. Phys. 42 (1993) 523.
[12] L. Néel, J. Phys. Radiat. 15 (1954) 376.
[13] C. Chappert, P. Bruno, J. Appl. Phys. 64 (1988) 5736.
[14] Yu.V. Goryunov, G.G. Khaliullin, I.A. Garifullin, L.R. Tagirov, F. Schreiber, P. Bödeker, Ch. Morawe, Th. Mü$^{+}$hge, H. Zabel, J. Appl. Phys. 76 (1994) 6096.
[15] F. Schreiber, Z. Frait, Th. Zeidler, N. Metoki, W. Donner, H. Zabel, J. Pelzl, Phys. Rev. B 51 (1995) 2920.